

Comparative Study of Five-Level and Seven-Level Inverter Controlled by Space Vector Pulse Width Modulation

Abdelmalik Bendaikha¹, Salah Saad²

¹Department of Electrical Engineering, Faculty of Technology, University Mouhamed Boudiaf, M'sila, Algeria.

²Laboratoire Systemes Electromécaniques (LSELM), University Badji-Mokhtar, Annaba, Algeria

Article Info

Article history:

Received Feb 3, 2017

Revised Apr 3, 2017

Accepted Apr 17, 2017

Keyword:

Harmonic distortion

Inverters topologies

SVPWM

Symmetrical sequence

Time response

ABSTRACT

This paper presents a MATLAB/SIMULINK model of two multi-level inverter topologies. Algorithms based on space vector modulation (SVM) technique are developed in order to conduct a comparative study on diode clamped five and seven level inverters. The scheme used to develop these control algorithms are based on symmetrical sequence because of the symmetry of the switching wave. Both topologies are simulated and analyzed using a squirrel cage induction motor. The results have showed that the best motor dynamic response with less harmonic distortion and torque fluctuations is obtained when seven-level inverter is employed.

Copyright © 2017 Institute of Advanced Engineering and Science.
All rights reserved.

Corresponding Author:

Abdelmalik Bendaikha,

Department of Electrical Engineering, Faculty of Technology,

University Mouhamed Boudiaf, M'sila, Algeria.

Email: malikbendaikha74@gmail.com

1. INTRODUCTION

Power Electronic Converters, especially DC/AC PWM inverters have been extending their range of use in industry because they provide reduced energy consumption, better system efficiency, improved quality of product, good maintenance, and so on. The voltage or current rating of the multilevel converter becomes a multiple of the individual switches, and so the power rating of the converter can exceed the limit imposed by the individual switching devices [1]. Variable speed drives applications require high performance, maximum reliability and minimum cost.

The use of static converters in variable speed drives is mainly due to the development of power semiconductors such as MOSFETs, IGBTs, GTOs. The association of inverters and AC machines rapidly became a standard in the industry of variable speed drive systems [2]-[4]. Furthermore, the development of pulse width modulation techniques as strategies to control voltage source inverters [5]-[6] has contributed to obtain an optimal operation of AC machines. The output voltage can be constant or variable with a constant or variable frequency. Thus, a variable output voltage is obtained by varying the input voltage and maintaining constant the inverter gain.

The desired voltage at the inverter output should be sinusoidal, however the shape of the wave in practice is non-sinusoidal, and rich in harmonics. Nevertheless, these harmonics can be minimized or reduced using multilevel inverters topologies with different pulse width modulation PWM techniques such as Space Vector PWM technique [2], [4], [5], [7].

In SVPWM, the three-phase stationary reference frame voltages for each inverter switching state are mapped to the complex two-phase orthogonal α - β plane. The DC voltage source of the inverter (AC/DC) can be a battery, a solar cell or any other type of DC voltage source. The output voltage of an inverter fed by a DC voltage source is an alternating voltage of rectangular shape. Filtering the voltage with rectangular

waveform enables its approximation to a sine wave. Therefore, the voltage to be filtered is at the industrial frequency, the filter will be expensive, and the results will be poor, hence the need to a technique for cutting an alternation in several pulses is required. However, the pulse width modulation (PWM) technique is introduced to overcome this issue.

This technique has several disadvantages such as high harmonic distortion, a phase voltage output limited to 87% of the DC voltage of the inverter, motor response time is long, the use of three reference voltages and difficult to be implemented on a DSP or microcontroller. There are three types of Multi Level Inverter, They are, Diode Clamped Multi Level Inverter, Capacitor Clamped Multi Level Inverter, Cascaded H-Bridge Multi Level Inverter [8].

In this work SVPWM algorithms are developed in order to compare the performances of diode clamped multilevel inverters (five and seven levels) in harmonics reduction, motor time response and torque fluctuations. The algorithms developed for these two topologies are tested on induction motor for validation. The obtained results have showed that harmonics are reduced to a lower value when seven levels inverter is used but the inverter commutation losses are less when five level inverters are used.

2. SVPWM THEORETICAL DEVELOPMENTS

The conventional two-level inverter is used for theoretical developments which can be extended for other multilevel inverters. It is assumed that the control of each arms of the inverter is complementary, thus as to replace static switches with two positions [5]-[6] Figure 1.

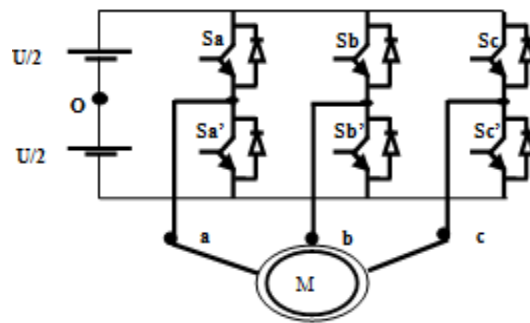


Figure 1. Conventional three phase inverter

Based on the concept of rotating vector, it can be considered that the inverter output is a voltage vector.

$$V_{ref0} = \sqrt{\frac{2}{3}} \times \left(V_{an0} + V_{bn0} \times e^{j \cdot \frac{2\pi}{3}} + V_{cn0} \times e^{j \cdot \frac{4\pi}{3}} \right) \quad (1)$$

The inverter switches are supposed to be ideal and can be represented as follows: S_j ($j=a, b, c$) such as, $S_j=1$ if phase a, is connected to the positive rail of the dc source, $S_j=0$ if phase a is connected to the negative rail of the DC source. The same principle is applied to the other two phases such as:

$$V_{ino} = S_j \cdot U - U/2 \quad (2)$$

The following Equation is obtained:

$$V_{ref} = \sqrt{\frac{2}{3}} \times \left(S_a + S_b \times e^{j \cdot \frac{2\pi}{3}} + S_c \times e^{j \cdot \frac{4\pi}{3}} \right) \quad (3)$$

The different combinations of S_a , S_b , S_c enable to generate eight possible vector positions V_{ref} with two positions corresponding to zero vector as shown in Figure 2.

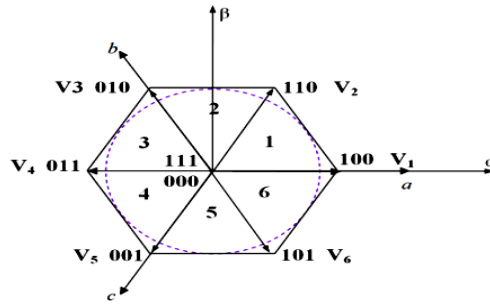


Figure 2. Inverter voltage vectors in (α-β) frame

The expressions of instantaneous phase and line to line inverter output voltages according to the upper switches can be established as follows:

$$\begin{bmatrix} V_{an} \\ V_{bn} \\ V_{cn} \end{bmatrix} = \frac{U}{3} \begin{bmatrix} 2 & -1 & -1 \\ -1 & 2 & -1 \\ -1 & -1 & 2 \end{bmatrix} \times \begin{bmatrix} S_a \\ S_b \\ S_c \end{bmatrix} \tag{4}$$

In order to simplify the computations and represent these voltages in a simplified form, the transformation of coordinates from the three phase stationary frame to α-β frame is applied respecting the power transfer transformation (Concordia transformation):

$$\begin{bmatrix} V_{s\alpha} \\ V_{s\beta} \end{bmatrix} = \sqrt{\frac{2}{3}} \begin{bmatrix} 1 & -\frac{1}{2} & -\frac{1}{2} \\ 0 & \frac{\sqrt{3}}{2} & -\frac{\sqrt{3}}{2} \end{bmatrix} \times \begin{bmatrix} V_{an} \\ V_{bn} \\ V_{cn} \end{bmatrix} \tag{5}$$

There are different control strategies enabling the determination of the three logic functions S_j (j=a, b, c). In this work SVPWM is used to develop the control strategy of the inverter.

2.1. Space Vector PWM Realization

SVPWM is largely used in modern control of induction motors to obtain sinusoidal waveforms at the inverter outputs [1], [4]-[7], [9]. Its basic principle is to reconstruct the voltage vector V_{ref} from the eight voltage vectors. Each vector corresponds to a switching state of a three phase voltage inverter switches. A reference voltage vector V_{ref} is evaluated approximately over a modulation period T_m . This vector is estimated in a sector by the application of adjacent voltage vectors and zero vectors V_8 and V_7 .

The computation of the reference voltage vector V_{ref} is obtained by analyzing all the switching states. The eight voltage vectors and the reference vector is represented in a αβ-plane. The switches being ON or OFF are determined by the location of the reference vector on this αβ-plane [10] Figure 3.

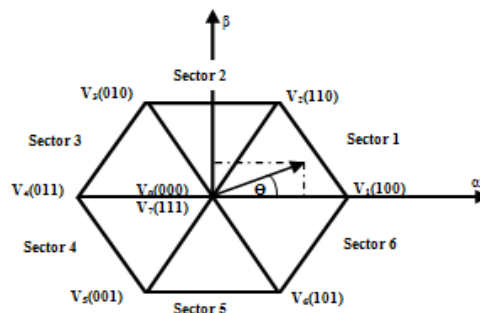


Figure 3. Representation of rotating vector in α-β frame

The SVPWM can be applied according to the following steps [5]-[6]:

- Determination of V_α , V_β , V_{ref} , and the rotating angle (θ).
- Application time of adjacent vectors x , y , and z .
- Determination of the switching time of each switch ($S_a, S_b, S_c, S_a', S_b'$ and S_c').

From Figure 4, V_α , V_β , V_{ref} , and the rotating angle (θ) can be determined as follows:

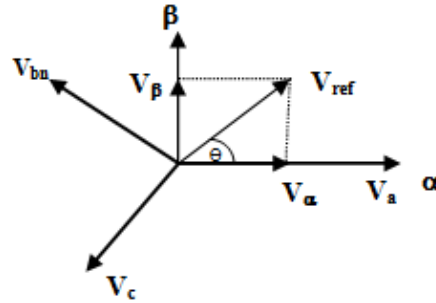


Figure 4. Voltage vector and its components in (α - β) frame

$$\begin{aligned} V_\alpha &= V_{an} - V_{bn} \cdot \cos 60 - V_{cn} \cos 60 \\ &= V_{an} - \frac{1}{2}V_{bn} - \frac{1}{2}V_{cn} \cos 60 \end{aligned}$$

$$\begin{aligned} V_\beta &= 0 \cdot V_{an} + V_{bn} \cdot \cos 30 - V_{cn} \cdot \cos 30 \\ &= 0 \cdot V_{an} - \frac{\sqrt{3}}{2}V_{bn} - \frac{\sqrt{3}}{2}V_{cn} \end{aligned}$$

Conserving the power transfer (Concordia transformation). The voltage vectors on the (α - β) axis can then be described as [10]:

$$\begin{bmatrix} V_{s\alpha} \\ V_{s\beta} \end{bmatrix} = \sqrt{\frac{2}{3}} \begin{bmatrix} 1 & -\frac{1}{2} & -\frac{1}{2} \\ 0 & \frac{\sqrt{3}}{2} & -\frac{\sqrt{3}}{2} \end{bmatrix} \times \begin{bmatrix} V_{an} \\ V_{bn} \\ V_{cn} \end{bmatrix} \quad (6)$$

$$V_{ref} = \sqrt{V_\alpha^2 + V_\beta^2} \quad (7)$$

$$\theta = \tan^{-1} \left(\frac{V_\beta}{V_\alpha} \right) = \omega t = 2\pi f t \quad (8)$$

Where:

f : is the fundamental frequency

The reference vector V_{ref} is estimated over a modulation period T_m , by generating an average vector determined by the application of inverter adjacent non-zero and zero vectors. Figure 4, illustrates the case where the reference vector is in sector 1. The application time of adjacent vectors are given as follows:

$$T_m = x + y + z \quad (9)$$

$$V_{ref} = \frac{x}{T_m} V_1 + \frac{y}{T_m} V_2 + \frac{z}{T_m} V_0 \quad (10)$$

The determination of 'x' and 'y' is obtained by the projection of the reference vector on α - β frame Figure 5.

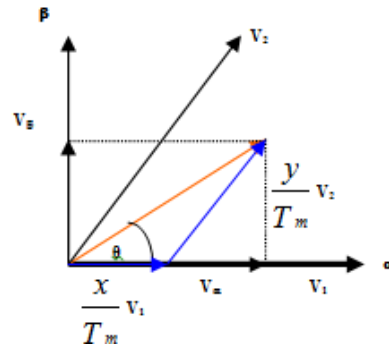


Figure 5. Projection of reference vector on α and β axis in sector 1

$$\int_0^{T_m} \mathbf{V}_{ref} dt = \int_0^x \mathbf{V}_{ref} dt + \int_x^{x+y} \mathbf{V}_{ref} dt + \int_{x+y}^{T_m} \mathbf{V}_{ref} dt$$

$$T_m \cdot \mathbf{V}_{ref} = (x \cdot \mathbf{V}_1 + y \cdot \mathbf{V}_2) + z \cdot (\mathbf{V}_7 \text{ ou } \mathbf{V}_8)$$

$$T_m \times |\mathbf{V}_{ref}| \begin{bmatrix} \cos(\theta) \\ \sin(\theta) \end{bmatrix} = x \cdot \sqrt{\frac{2}{3}} U \begin{bmatrix} 1 \\ 0 \end{bmatrix} + y \cdot \sqrt{\frac{2}{3}} U \begin{bmatrix} \cos(\frac{\pi}{3}) \\ \sin(\frac{\pi}{3}) \end{bmatrix} \quad (11)$$

Where, $(0 \leq \theta \leq 60^\circ)$

$$x = T_m \times \frac{|\mathbf{V}_{ref}|}{\sqrt{\frac{2}{3}} U} \cdot \frac{\sin(\frac{\pi}{3} - \theta)}{\sin(\frac{\pi}{3})} \quad (12)$$

$$y = T_m \times \frac{|\mathbf{V}_{ref}|}{\sqrt{\frac{2}{3}} U} \cdot \frac{\sin(\theta)}{\sin(\frac{\pi}{3})} \quad (13)$$

In order to apply the SVPWM technique to a five and seven level voltage source inverter a control algorithm is developed using symmetrical sequence.

3. FIVE-LEVEL INVERTER

Diode clamped five-level inverter has three symmetrical arms each consisting of eight bidirectional switches in series. These switches must not be ON or OFF simultaneously in order to avoid the short circuit of the inverter dc source. Each switch consists of a bi-commutable semiconductor and a diode connected in anti-parallel. The number of diodes is six by arm ensure the application of different voltage levels at the output of each arm. Each arm is connected to a dc supply of electromotive force ($4U_c$), these four generators are equal. This inverter is five-level because it delivers five voltage levels per arm ($U/2, U/4, 0, -U/4, -U/2$).

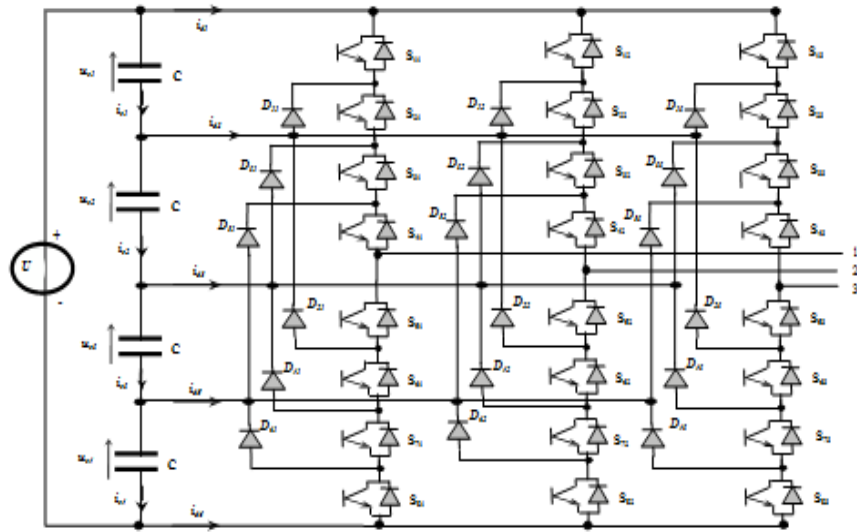


Figure 6. Five-level inverter topology

3.1. Switching Functions

For each switch $S_{ij} (i = \overline{1-8}, j = \overline{1-3})$, a switching function F_{ij} is defined as follows:

$$F_{ij} = \begin{cases} 1 & \text{if } S_{ij} \text{ is ON} \\ 0 & \text{if } S_{ij} \text{ is OFF} \end{cases} \tag{18}$$

The switches of the lower-half arm are complementary with the switches of upper half-arm

$$F_{ij} = 1 - F_{(i-4)j}, i = \overline{5-8}; j = \overline{1-4} \tag{19}$$

Table 1. Switching State of One Inverter Arm

State	S_{1x}	S_{2x}	S_{3x}	S_{4x}	S_{5x}	S_{6x}	S_{7x}	S_{8x}	V_{0x}
4	1	1	1	1	0	0	0	0	$U/2$
3	0	1	1	1	1	0	0	0	$U/4$
2	0	0	1	1	1	1	0	0	0
1	0	0	0	1	1	1	1	0	$-U/4$
0	0	0	0	0	1	1	1	1	$-U/2$

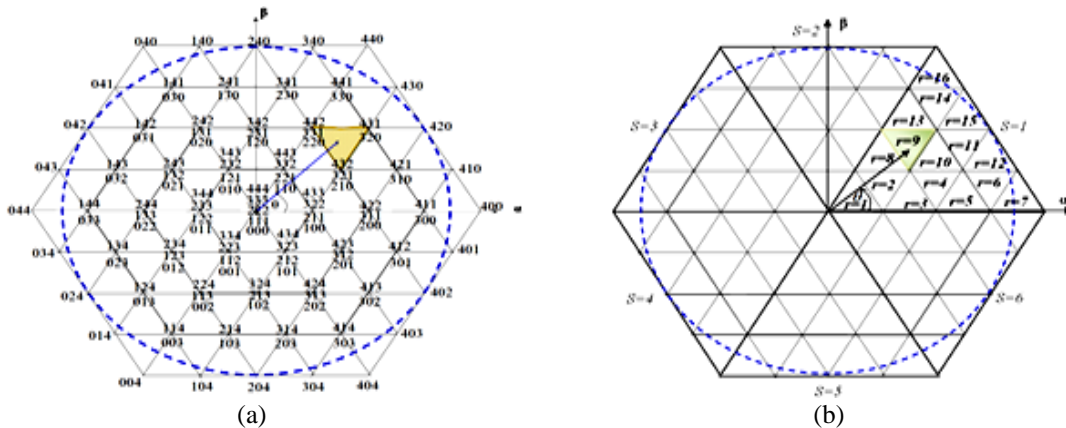


Figure 7. (a) Space vector diagram of five-level inverter (b) Sectors and regions of space vector diagram

4. SEVEN-LEVEL INVERTER

The seven-level inverter has three symmetrical arms each consisting of (12) bidirectional switches in series. These switches must not be ON or OFF simultaneously to prevent the short circuit of the dc inverter input, or the opening of load inductive circuit. Each switch consists of a bi-commutable semiconductor and a diode connected in anti-parallel. The number of diodes is 10 by arm ensure the application of different voltage levels at the output of each arm. Each arm is connected to a dc supply of electromotive force (6Uc), these six generators are equal. This inverter is seven-level because it provides seven voltage levels per arm (U/2, U/4, U/6, 0, -U/6, -U/4, -U/2).

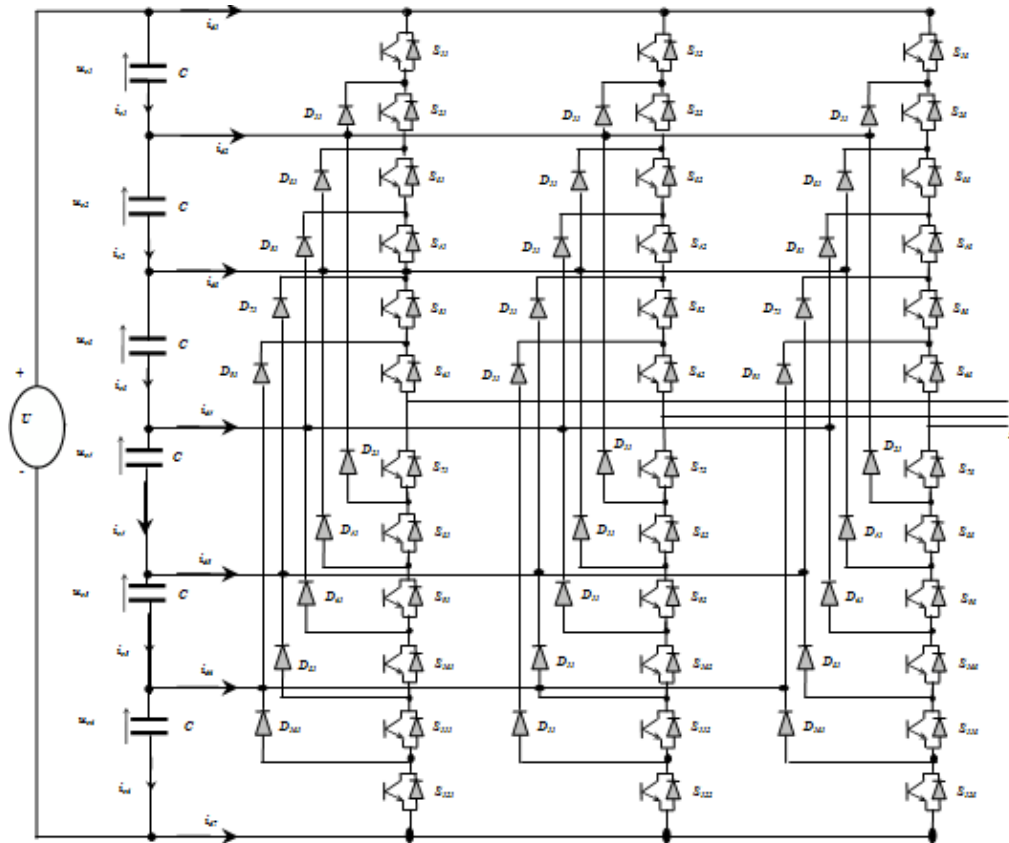


Figure 8. Structure of seven-level floating diodes inverter

4.1. Switching Functions

$$F_{ij} = \begin{cases} 1 & \text{if } S_{ij} \text{ is ON} \\ 0 & \text{if } S_{ij} \text{ is OFF} \end{cases} \tag{20}$$

$$F_{ij} = 1 - F_{(i-6)j} \quad i = \overline{7-12} \quad j = \overline{1-3} \tag{21}$$

Table 2. Switching State of the Inverter Arm

St	S _{1x}	S _{2x}	S _{3x}	S _{4x}	S _{5x}	S _{6x}	S _{7x}	S _{8x}	S _{9x}	S _{10x}	S _{11x}	S _{12x}	V _{0x}
6	1	1	1	1	1	1	0	0	0	0	0	0	U/2
5	1	1	1	1	1	0	1	0	0	0	0	0	U/4
4	1	1	1	1	0	0	1	1	0	0	0	0	U/6
3	1	1	1	0	0	0	1	1	1	0	0	0	0
2	1	1	0	0	0	0	1	1	1	1	0	0	-U/6
1	1	0	0	0	0	0	1	1	1	1	1	0	-U/4
0	0	0	0	0	0	0	1	1	1	1	1	1	-U/2

5. COMPUTER SIMULATION

The simulation is conducted with five level and seven level inverter controlled by SPWM technique using parameters presented in Table 3. The results of simulation of SVPWM voltage source inverter for both topologies feeding an induction motor with amplitude modulation index $r=0.866$ and frequency modulation $m=96$ are presented and compared. Motor technical parameters are presented in the Table 3 presented below.

Table 3. Motors Parameters

Parameters	Values
Motor power	$P_n = 1.5 \text{ Kw}$
Nominal frequency	$F = 50 \text{ Hz}$
pole pair Number	$P=2$
Supply voltage	$u_n = 220 \text{ v} / 380 \text{ v}$
Nominal current	$I_n = 6.2 / 3.7 \text{ A}$
Nominal rotational speed	$n_n = 1420 \text{ tr/min}$
Stator resistance	$R_s = 4.85 \ \Omega$
Rotor resistance	$R_r = 3.805 \ \Omega$
Stator inductance	$L_s = 0.2740 \text{ H}$
Rotor inductance	$L_r = 0.2740 \text{ H}$
Mutual inductance	$M_{sr} = 0.2580 \text{ H}$
moment of inertia	$J = 0.031 \text{ Kg m}^2$
Friction coefficient	$f_t = 0 \text{ Kg m}^2/\text{s}$

Several operation characteristics were studied, such as reference vector angle and reference vector displacement between sectors and regions. Furthermore some internal variables, such as stator current, phase to neutral voltage, line to line voltage and their frequency spectrum are measured. To show the robustness of this control strategy the torque and the speed were viewed using Matlab simulink Blocks. For simulation tests the initial torque value was set to 0 Nm and after 0.6 s, this torque was increased to 15 N.m. The obtained results when five level inverter is used are given below Figure 9(a) to 9(k).

5.1. Results of Five-Level Inverter Fed Induction Motor

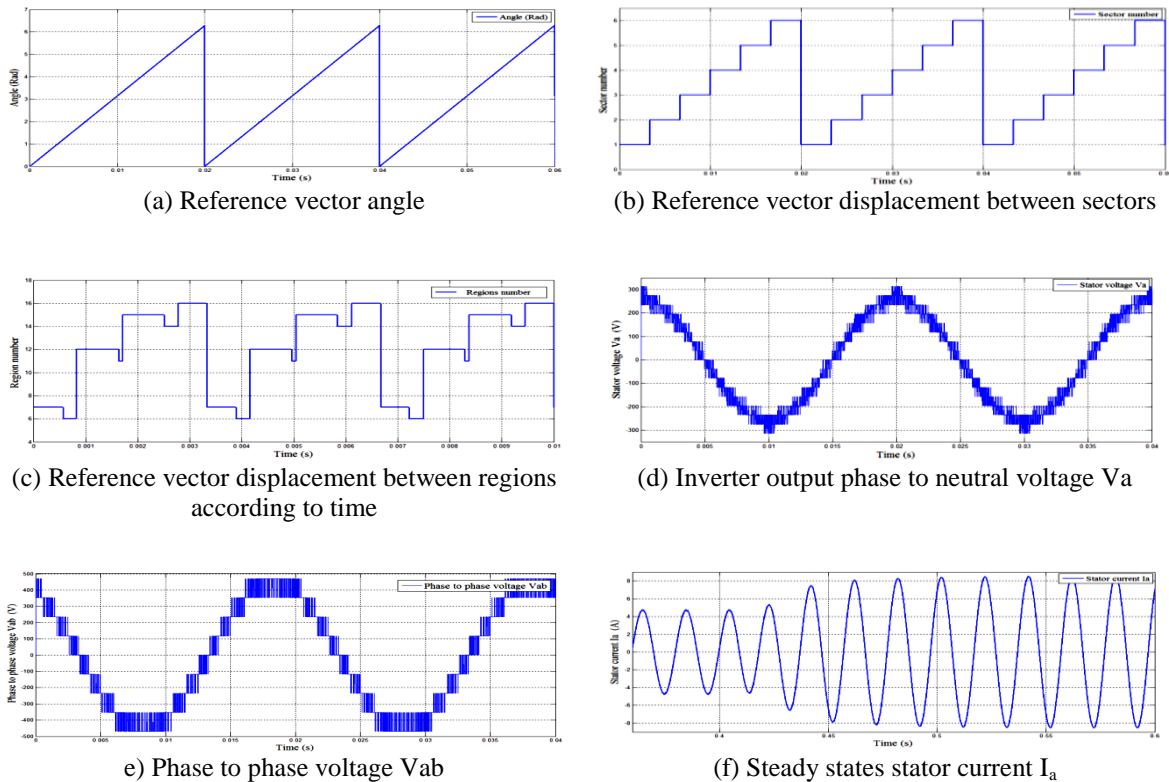


Figure 9. The results of five level inverter, for $r=0.886$, $m=96$

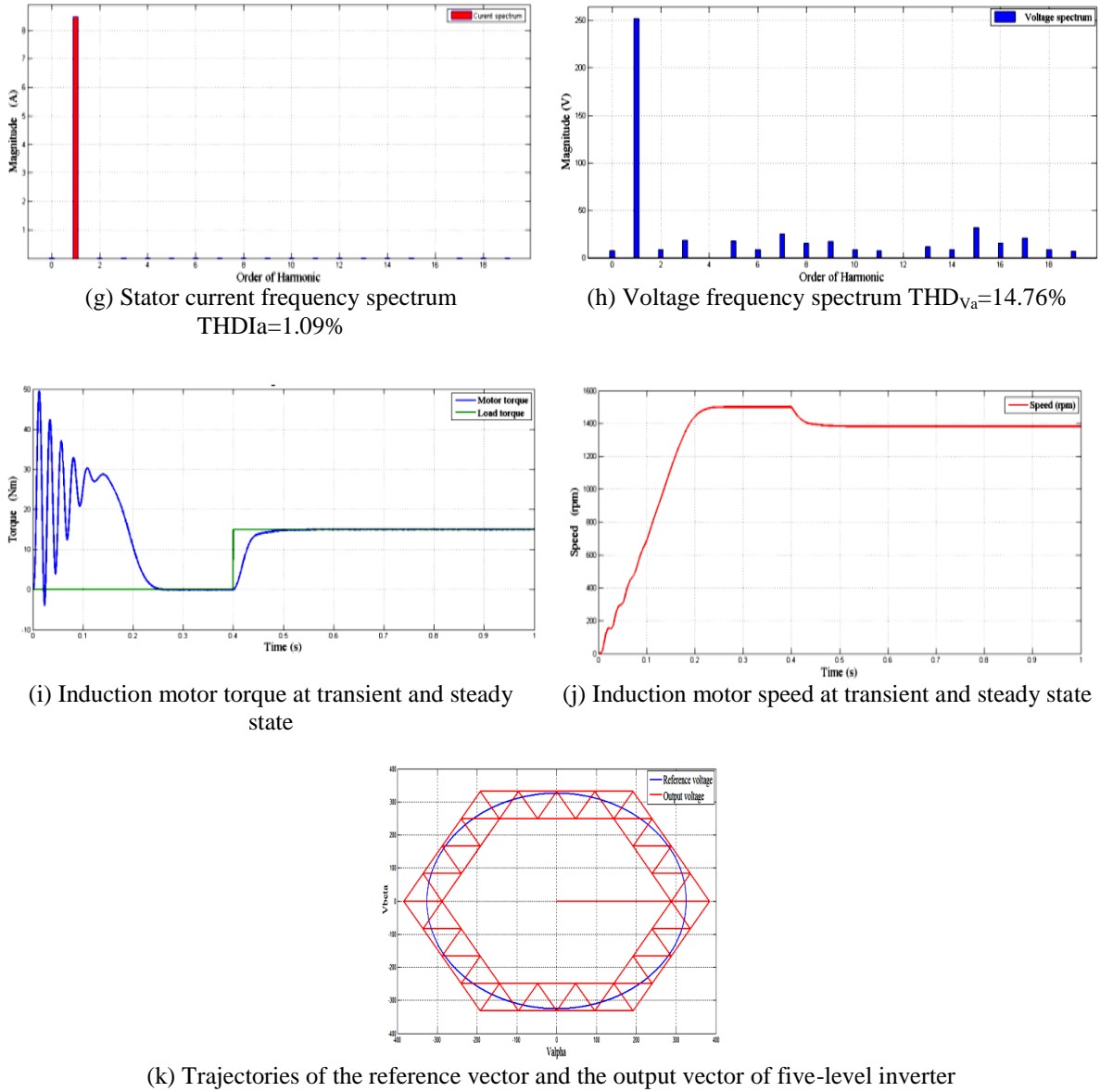


Figure 9. The results of five level inverter, for $r=0.886$, $m=96$

5.2. Results of Seven-Level Inverter Fed Induction Motor

The obtained results when seven level inverter is used are given below Figure 10(a) to 10(k).

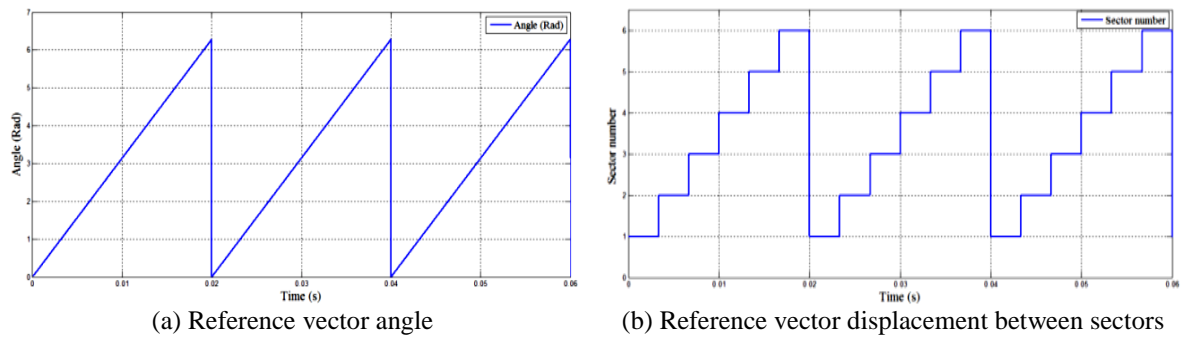
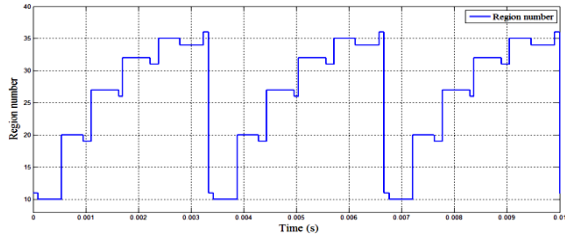
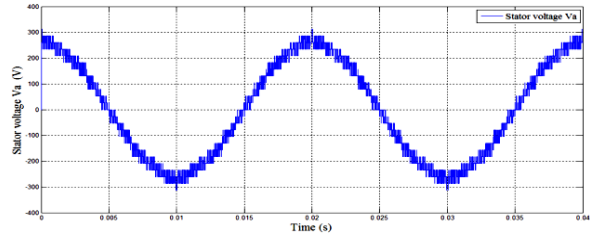


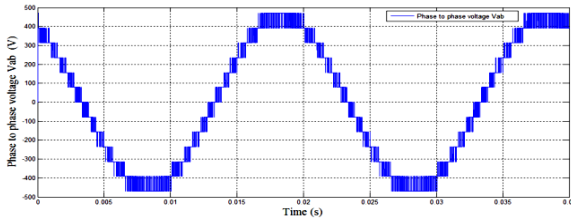
Figure 10. The results of seven level inverter, for $r=0.886$, $m=96$



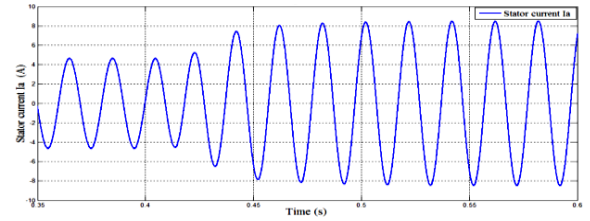
(c) Reference vector displacement between regions according to time



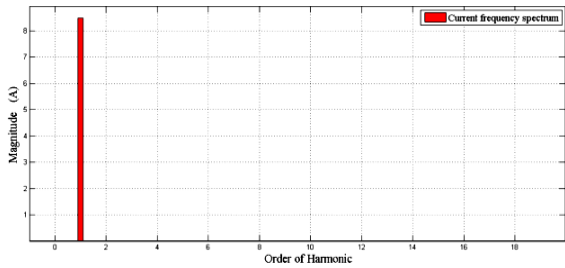
(d) Inverter output phase to neutral voltage V_a



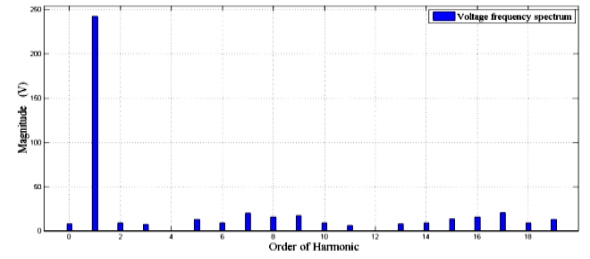
e) Phase to phase voltage Vab



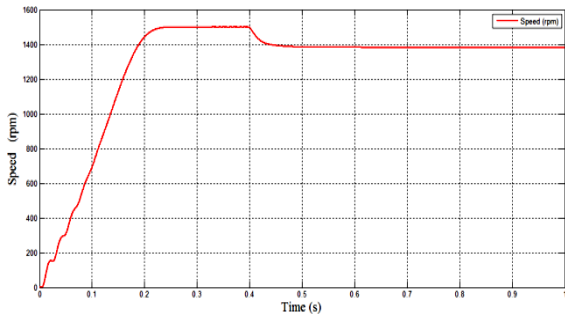
(f) Steady states stator current I_a



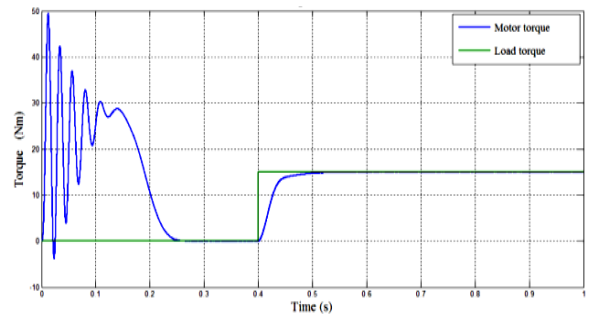
(g) Stator current frequency spectrum $THDI_a=0.25\%$



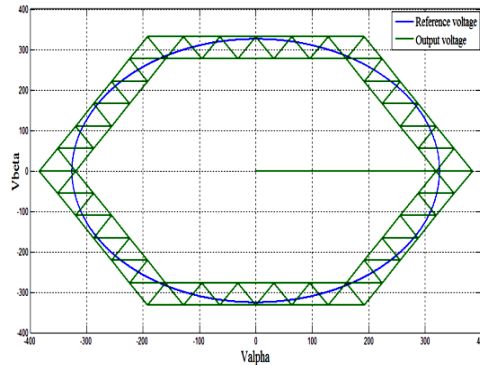
(h) Voltage frequency spectrum $THDV_a=9.37\%$



(i) Induction motor speed at transient and steady state



(j) Induction motor torque at transient and steady state



(k) Trajectories of the reference voltage and the output voltage of seven-level inverter

Figure 10. The results of seven level inverter, for $r=0.886$, $m=96$

6. RESULTS AND ANALYSIS

The results of the developed algorithm of a five level inverter controlling induction motor are illustrated in Figure 9(a) to Figure 9(k). The Figure 9(a, b and c) illustrate reference vector angle, reference vector displacement between sectors and reference vector displacement between regions according to time respectively.

The phase to neutral voltage (Figure 9(d)), the stator phase current (Figure 9(f)) waveforms and their frequency spectrum illustrated on Figure 9(g) and Figure 9(h) have THD values equal to (14.76%) and (1.09%) respectively for an amplitude modulation index $r=0.866$ and a frequency modulation $m=96$. Figure 9.e illustrates phase to phase voltage V_{ab} . Figure 9(k) illustrate Trajectories of the reference vector and the output vector. The speed curve shown in Figure 9(i) has three sections; transient state section from 0 to 0.29 s, no load operation section from 0.29-0.4 s and a section for load (15 N.m) operation applied at 0.4 s and the time response is less than 0.15s.

The torque curve presented in Figure 10.j) has three sections; transient state section from 0 to 0.29 s, no load (0.00 N.m) operation section from 0.29-0.4 s and a section for load (15 N.m) operation applied at 0.4 s and the time response is less than 0.15s. Phase to neutral voltage (Figure 9(d)) has seventeen voltage levels and phase to phase voltage has nine voltage levels, thus its shape is closer to the sinusoidal shape. Figure 9(k) illustrates trajectories of the reference vector and the output vector showing that the output vector is tracking the reference vector.

The results when the developed algorithm of a seven level inverter controlling induction motor is applied are presented in Figure 10(a) to Figure 10(k). The Figure 10(a, b, and c) illustrate reference vector angle, reference vector displacement between sectors and reference vector displacement between regions according to time, respectively. Figure 10.e illustrates phase to phase voltage V_{ab} . The phase to neutral voltage (Figure 10.d), the stator phase current (Figure 10(f)) waveforms and their frequency spectrum illustrated on Figure 10(h) and Figure 10(g) have THD values equal to (9.37%) and (0.25%) respectively for an amplitude modulation index $r=0.866$ and a frequency modulation $m=96$.

The speed curve shown in Figure 10.i has three sections; transient state section from 0 to 0.25 s, no load operation section from 0.25-0.4 s and a section for load (15 N.m) operation applied at 0.4 s and the time response is less than 0.12s. The torque curve presented in Figure 10(j) has three sections; transient state section from 0 to 0.25 s, no load (0.00 N.m) operation section from 0.25-0.4 s and a section for load (15 N.m) operation applied at 0.4 s and the time response is less than 0.12s.

Phase to neutral voltage has twenty five voltage levels (Figure 10.d) and phase to phase voltage has thirteen voltage levels. It can be observed that speed and torque time responses are better when the motor is fed by seven-level inverter. Therefore, a better speed regulation is obtained. The inverter output current waveform of seven-level inverter is almost sinusoidal contains less harmonics and less torque fluctuations thus, a better motor dynamic response is obtained. Figure 10(k) illustrate Trajectories of the reference vector and the output vector showing that the output vector is tracking the reference vector.

In order to evaluate the SVPWM strategy applied to five and seven level inverter topologies, the speed and torque curves as well as current and voltage frequency spectrums are compared. The phase to neutral voltage, the stator phase current waveforms and the frequency spectrum of five level inverter have THD values equal to (14.76%) and (1.09%) respectively. The phase to neutral voltage, the stator phase current waveforms and frequency spectrum of seven level inverter have THD values equal to (9.37%) and (0.25%) respectively. The results have showed that when seven level inverter is used the harmonic currents and voltage distortions are reduced and torque fluctuations are less. But the developed algorithm gives reduced commutation losses when five-level inverter is used because the switching devices number is reduced. Comparing these results to the results of the literature it can be noticed that THD values of both current and voltage are well below the obtained values of [1], [11] and IEEE recommendations.

7. CONCLUSION

The present paper has presented a comparative study of multilevel inverter topologies controlled by space vector PWM feeding an induction motor. The results have showed that seven level inverter gives reduced harmonics current and voltage distortion and less torque fluctuations. But the commutation losses are minimized when five-level inverter because the switching devices number is reduced.

The results have showed that the seven-level inverter is the best topology compared to five-level topology; but it has some disadvantages such as large number of semiconductor devices which involves high losses compared to other types. This work has allowed understanding the basic principles to design and simulation of any complex power engineering system. It has served to enhance knowledge of programming, modeling and power control techniques of induction motors.

REFERENCES

- [1] Chetanya Gupta, Devbrat Kuanr, Abhishek Varshney, Tahir Khurshaid, Kapil Dev Singh " Harmonic Analysis of Seven and Nine Level Cascade Multilevel Inverter using Multi-Carrier PWM Technique", *IJPEDS*, Vol. 5, No. 1, July 2014, pp. 76~82.
- [2] Ayşe Kocalmıř, Sedat Sünter, "Simulation of a Space Vector PWM Controller For a Three-Level Voltage-Fed Inverter Motor Drive", 2006 *IEEE*, pp 1915-1920.
- [3] Samir Kouro, Rafael Bernal, Hernan Miranda, Jose Rodríguez and Jorge Pontt, "Direct Torque Control With Reduced Switching Losses for Asymmetric Multilevel Inverter Fed Induction Motor Drives", 2006 *IEEE*, pp 2441-2446.
- [4] Fouad Berrabaha, Saad Salah, Ali Chebabhi, "SVM technique based on DTC sensorless control optimized by ANN applied to a double stator asynchronous machine fed by three-level six-phase inverter", *The Mediterranean Journal of Measurement and Control*, Vol. 12, No. 2, 2016.
- [5] Keliang Zhou and Danwei Wang, "Relationship Between Space-Vector Modulation and Three-Phase Carrier-Based PWM", *IEEE transactions on industrial electronics*, vol. 49, no. , February 2002.
- [6] K.S. Gayathri Devi, S. Arun, C. Sreeja, "Comparative study on different five level inverter topologies", *Electrical Power and Energy Systems* 63 (2014) 363–372.
- [7] Mohammad Shadab Mirza, Tufail Mohammad, Qamar Alam, Mohammad Ariffuddin Mallick, "Simulation and Analysis of a Grid Connected Multi-level Converter Topologies and their Comparison", *Journal of Electrical Systems and Information Technology I* (2014) 166–174.
- [8] S. Umashankar, T. S. Sreedevi, V. G. Nithya, and D. Vijayakumar, "A New 7-Level Symmetric Multilevel Inverter with Minimum Number of Switches", Volume 2013, Article ID 476876, 9 pages.
- [9] M. Valan Rajkumar, P.S. Manoharan, A. Ravi, "Simulation and an experimental investigation of SVPWM technique on a multilevel voltage source inverter for photovoltaic systems", *Electrical Power and Energy Systems ScienceDirect*, Volume 52, November 2013, Pages 116–131.
- [10] Gomathi C, Navya Nagath, Veerakumar S, "Sampled Reference Frame Algorithm Based on Space Vector Pulse Width Modulation for Five Level Cascaded H-Bridge Inverter", *Bulletin of Electrical Engineering and Informatics* Vol. 3, No. 2, June 2014, pp. 127~140.
- [11] Zulkifilie Bin Ibrahim et al, "Comparative Analysis of PWM Techniques for Three Level Diode Clamped Voltage Source Inverter ", *International Journal of Power Electronics and Drive System (IJPEDS)* Vol. 5, No. 1, July 2014, pp. 15~23.

BIOGRAPHIES OF AUTHORS



Abdelmalik Bendaikha was born in Batna, Algeria, in 1974. He received the Engineer, master's degrees in electromechanical applied to mining fields from Badji-Mokhtar Annaba, Algeria, in 1997, 2007, respectively. Since 2007, he is a Senior Lecturer with the University of M'sila Algeria. His research interests are mainly in the area of Measurement, Control, Electronics & electrical drives



Salah Saad was born in Batna, Algeria, in 1958. He received the Engineer degree in electromechanical applied to mining fields from Badji-Mokhtar Annaba University Algeria and the Ph.D. degree from Nottingham University, U.K., in 1983 and 1988, respectively. Since 1988, he has been a Lecturer, Senior Lecturer, and Professor with Badji-Mokhtar Annaba University Algeria. He has supervised many graduated and postgraduate student thesis. He has conducted many researches projects in power electronics applications, electrical ac and dc drives as well as diagnosis and faults detection in ac machines. His research interests are mainly in the area of power electronics such as harmonics elimination by active filters, PWM and space vector modulation control, multilevel inverters, new converter topologies, and vibration sensors. He has authored or co-authored many journal and conference papers. He has co-authored a book in the field of signal processing published in Algeria in 1992.